NEUROSCIENCE

Neuronal FAM171A2 mediates α-synuclein fibril uptake and drives Parkinson's disease

Kai-Min Wu[1], Qian-Hui Xu[2,3], Yi-Qi Liu[1], Yi-Wei Feng[1], Si-Da Han[1], Ya-Ru Zhang[1], Shi-Dong Chen[1], Yu Guo[1], Bang-Sheng Wu[1], Ling-Zhi Ma[4], Yi Zhang[1], Yi-Lin Chen[1], Liu Yang[1], Zhao-Fei Yang[5], Yu-Jie Xiao[6], Ting-Ting Wang[7], Jue Zhao[1], Shu-Fen Chen[1], Mei Cui[1], Bo-Xun Lu[8], Wei-Dong Le[5,9], You-Sheng Shu[6], Keqiang Ye[10,11], Jia-Yi Li[12,13], Wen-Sheng Li[14], Jian Wang[1], Cong Liu[2,15,16]*, Peng Yuan[1,17]*, Jin-Tai Yu[1]*

Neuronal accumulation and spread of pathological α-synuclein (α-syn) fibrils are key events in Parkinson's disease (PD) pathophysiology. However, the neuronal mechanisms underlying the uptake of α-syn fibrils remain unclear. In this work, we identified *FAM171A2* as a PD risk gene that affects α-syn aggregation. Overexpressing FAM171A2 promotes α-syn fibril endocytosis and exacerbates the spread and neurotoxicity of α-syn pathology. Neuronal-specific knockdown of FAM171A2 expression shows protective effects. Mechanistically, the FAM171A2 extracellular domain 1 interacts with the α-syn C terminus through electrostatic forces, with >1000 times more selective for fibrils. Furthermore, we identified bemcentinib as an effective blocker of FAM171A2–α-syn fibril interaction with an in vitro binding assay, in cellular models, and in mice. Our findings identified FAM171A2 as a potential receptor for the neuronal uptake of α-syn fibrils and, thus, as a therapeutic target against PD.

Parkinson's disease (PD) is a neurodegenerative disorder affecting motor and cognitive functions (*1*–*3*). Aggregations of pathological α-synuclein (α-syn) in various brain regions mediate the progression of the disease (*4*, *5*). Aggregated α-syn proteins form fibrils that act in a prion-like manner, spreading α-syn pathology in various regions of the brain (*6*, *7*). However, the molecular mechanism underlying the interneuronal transmission remains unknown.

Previous studies indicated that the pathological α-syn is internalized by endocytosis (*8*, *9*) with different receptors (*10*–*12*); however, the specific receptors on neurons remain to be fully identified. We previously reported that the single-nucleotide polymorphism rs708384 of *FAM171A2* is associated with an increased risk for PD (*13*). The amount of FAM171A2 in the cerebrospinal fluid (CSF) is increased in individuals with PD and correlates with indications of high α-syn aggregations in the brain (Fig. 1). In this study, we hypothesized that FAM171A2 may be involved in the interneuronal spread of α-syn pathology. We systematically tested this hypothesis by using a mouse model of α-syn pathology propagation. We established a causal relationship between FAM171A2 expression and neuronal uptake of α-syn fibrils as well as its downstream neurotoxicity. Combining biochemical and structural approaches, we identified the biophysical basis underlying the FAM171A2–α-syn interaction. We further found that a small molecule, bemcentinib, blocked this interaction in cultured cells and in vivo. Taken together, our data revealed that FAM171A2 is a specific mediator for α-syn fibril internalization and that antagonizing this interaction may represent a therapeutic target against α-syn propagation in PD.

[1]Department of Neurology and National Center for Neurological Diseases, Huashan Hospital, State Key Laboratory of Medical Neurobiology and Ministry of Education Frontiers Center for Brain Science, Shanghai Medical College, Fudan University, Shanghai, China. [2]Interdisciplinary Research Center on Biology and Chemistry, Shanghai Institute of Organic Chemistry, Chinese Academy of Sciences, Shanghai, China. [3]University of Chinese Academy of Sciences, Beijing, China. [4]Department of Neurology, Qingdao Municipal Hospital, Qingdao University, Qingdao, China. [5]Liaoning Provincial Key Laboratory for Research on the Pathogenic Mechanisms of Neurological Diseases, The First Affiliated Hospital of Dalian Medical University, Dalian, China. [6]Department of Neurology, Huashan Hospital, State Key Laboratory of Medical Neurobiology, Institute for Translational Brain Research, MOE Frontiers Center for Brain Science, Fudan University, Shanghai, China. [7]Department of Pharmacy, Huashan Hospital, Fudan University, Shanghai, China. [8]Neurology Department at Huashan Hospital, State Key Laboratory of Medical Neurobiology and MOE Frontiers Center for Brain Science, Institutes of Brain Science, School of Life Sciences, Fudan University, Shanghai, China. [9]Institute of Neurology, Sichuan Provincial People's Hospital, Medical School of University of Electronic Science and Technology of China, Chengdu, China. [10]Department of Pathology and Laboratory Medicine, Emory University School of Medicine, Atlanta, GA, USA. [11]Faculty of Life and Health Sciences, Shenzhen Institute of Advanced Technology, Chinese Academy of Sciences, Shenzhen, Guangdong, China. [12]Neural Plasticity and Repair Unit, Department of Experimental Medical Science, Wallenberg Neuroscience Center, Lund University, Lund, Sweden. [13]Institute of Health Sciences, China Medical University, Liaoning, Shenyang, China. [14]Department of Anatomy, Histology and Embryology, School of Basic Medical Sciences, State Key Laboratory of Medical Neurobiology, MOE Frontiers Center for Brain Science, Institutes of Brain Science, Fudan University, Shanghai, China. [15]State Key Laboratory of Small Molecule Modulation of Biological Processes, Shanghai Institute of Organic Chemistry, University of Chinese Academy of Sciences, Shanghai, China. [16]Shanghai Academy of Natural Sciences (SANS), Fudan University, Shanghai, China. [17]Department of Rehabilitation Medicine, Huashan Hospital, State Key Laboratory of Medical Neurobiology, Institute for Translational Brain Research, MOE Frontiers Center for Brain Science, MOE Innovative Center for New Drug Development of Immune Inflammatory Diseases, Fudan University, Shanghai, China.
*Corresponding author. Email: liulab@sioc.ac.cn (C.L.); pyuan@fudan.edu.cn (P.Y.); jintai_yu@fudan.edu.cn (J.-T.Y.)

Increased FAM171A2 expression correlates with α-syn pathology in samples from individuals with PD

We previously reported that *FAM171A2* rs708384 is associated with the risk of PD (*13*). To further characterize the associations between all common variants of *FAM171A2* and PD risk, we performed a large meta–genome-wide association study (GWAS) in PD using data from more than 1 million total participants. Our analyses revealed significant associations between PD risk and five variants of *FAM171A2*: rs850738 [odds ratio (OR) = 1.05, $P = 1.95 \times 10^{-9}$], rs708383 (OR = 1.05, $P = 4.97 \times 10^{-9}$), rs708384 (OR = 1.05, $P = 5.38 \times 10^{-9}$), rs71371993 (OR = 1.10, $P = 4.74 \times 10^{-6}$), and rs35941271 (OR = 1.08, $P = 5.93 \times 10^{-5}$) (Fig. 1A and table S1). We then performed immunohistochemical staining of FAM171A2 in postmortem human brain tissues and found neuronal staining in the midbrain taken from four healthy brains (controls) and two brains from patients with PD, with particularly high signal observed on the plasma membrane (Fig. 1B). We observed elevated FAM171A2 expression in patients with PD compared with controls (Fig. 1C). Transcriptional analysis further showed that FAM171A2 is expressed in the dopaminergic neurons of the substantia nigra (SN) as well as in other cell types across different regions (fig. S1).

We then collected CSF samples from 30 patients with PD and 30 age- and sex-matched controls and evaluated their FAM171A2 expression by immunoreactivity-based dot blot (Fig. 1D and table S2). We found that patients with PD had elevated amount of FAM171A2 in CSF compared with controls (Fig. 1E), which was validated by analyzing data from a larger cohort of 517 PD cases and 169 controls, obtained from the Parkinson's Progression Markers Initiative (PPMI) cohort (Fig. 1F and table S3). We next examined the correlation between FAM171A2 and α-syn in the CSF of individuals with PD. Consistent with previous reports (*14*), we observed reduced total α-syn expression in individuals with PD in both cohorts (fig. S2, A to D), suggesting increased accumulation of α-syn aggregates in the brain. We also found a significant negative correlation between FAM171A2 and CSF α-syn expression among individuals with PD in the PPMI cohort ($\beta = -0.38$, $P = 1.39 \times 10^{-15}$; Fig. 1G). These results suggested a correlation between elevated FAM171A2 and α-syn aggregation in the brain. Furthermore, the PPMI cohort measured pathological α-syn seed using a fluorescence-based amplification assay (SAA) and showed that higher FAM171A2 expression correlated with shorter times to reach threshold for detection ($\beta = -0.17$, $P = 0.001$; Fig. 1H) or 50% of the maximum fluorescence ($\beta = -0.18$, $P = 0.001$; Fig. 1I) in patients with PD, indicating an association of higher FAM171A2 expression with increased amounts of pathological α-syn seeds. We controlled for the potential

A

FAM171A2 meta-analysis (12 overlapping SNPs)

UKB	+	Chang 2017, Stage1	+	Finngen
11,324 PD+proxy cases 188,484 controls		20,184 PD cases 397,324 controls		4,681 PD cases 407,500 controls

Marker Name	Pos	Effect Allele	Reference Allele	Freq	Meta-P	PD risk odds Ratio
rs850738	42434630	G	A	0.427	1.95×10^{-9}	1.05
rs708383	42437754	A	G	0.392	4.97×10^{-9}	1.05
rs708384	42437682	A	C	0.392	5.38×10^{-9}	1.05
rs71371993	42437000	A	G	0.099	4.74×10^{-6}	1.10
rs35941271	42436220	A	G	0.116	5.93×10^{-5}	1.08

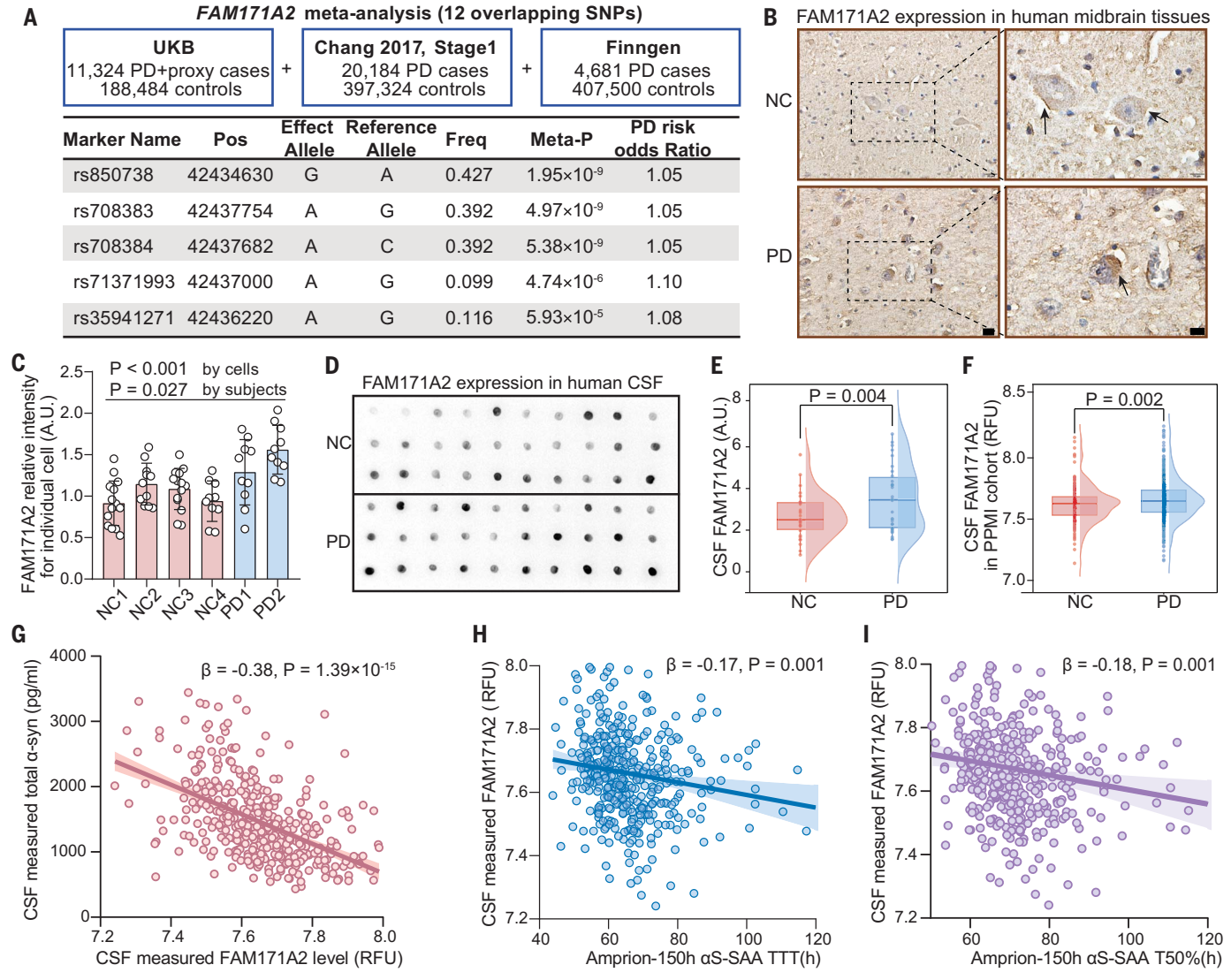

Fig. 1. Elevated FAM171A2 expression correlates with α-syn pathology in patients with PD. (**A**) Associations between *FAM171A2* variants and PD risk. Chang 2017 refers to reference (*34*). (**B**) Immunohistochemical images of FAM171A2 protein expression in human midbrain tissues. The insets show examples of higher magnification in the dashed rectangles. Arrows indicate heightened staining of FAM171A2. Scale bar, 20 μm. NC, normal control. (**C**) Quantification of FAM171A2 expression in (B) by average optical density measurement (N = 10 to 15 cells). Data are expressed as means ± SEM and were tested with one-way analysis of variance (ANOVA) by cells and unpaired t test by subjects. A.U., arbitrary units. (**D**) Representative dot blot image of FAM171A2 expression in CSF samples from sporadic PD patients (N = 30) and age- and sex-matched neurological NCs (N = 30). (**E**) Densitometric analysis of FAM171A2 amounts in PD patients and NCs. Boxplots depict the median and 25th and 75th quartiles, whereas whiskers represent the full range. Statistical significance was determined with an unpaired t test. (**F**) CSF FAM171A2 amounts in PD patients and NCs from PPMI cohort. Boxplots depict the median and 25th and 75th quartiles, and whiskers represent the full range. Statistical significance was determined by using regression models adjusted for sex and age. RFU, relative fluorescence units. (**G** to **I**) Scatterplots showing the correlation between FAM171A2 and total α-syn amounts in CSF (G), the time to threshold (TTT) of α-syn SAA (αS-SAA) (H), and the time to 50% max fluorescence (T50%) of α-syn SAA (I) in patients with PD. Measurements in (G) to (I) were adjusted for age, sex, and progranulin expression. Linear trend lines are shown, and the 95% confidence intervals are indicated by shading. Coefficients of determination (R^2) are 0.29 (G), 0.07 (H), and 0.06 (I). Estimate regression coefficients (β) and P values are shown. UKB, UK Biobank; Meta-P, P value for meta-analysis; SNPs, single-nucleotide polymorphisms; Pos, the chromosomal position in base pairs according to the human genome build hg19; Freq, frequency; NC, neurological normal control; PPMI, Parkinson's Progression Markers Initiative cohort; h, hours.

confounding effect of progranulin (*13*). The progranulin expression in CSF showed no reduction in individuals with PD compared with controls (fig. S2, E to H). Thus, elevation of FAM171A2 is associated with α-syn aggregation in the brain, potentially contributing to PD pathogenesis.

FAM171A2 controls preformed-fibril inoculation–induced α-syn pathology and neurotoxicity

To test the causal effect of FAM171A2 on α-syn pathology, we used a mouse model with intrastriatal inoculation of recombinant α-syn preformed fibrils (α-syn PFFs). Inoculation of α-syn PFFs leads to a time-dependent accumulation of misfolded α-syn pathology in the interconnected brain regions (*4*, *15*, *16*). This approach allowed us to dissect the specific process of pathogenic α-syn propagation. We visualized the fibrils formed from α-syn monomers with transmitted electron microscopy (fig. S3A) and confirmed the multimeric forms

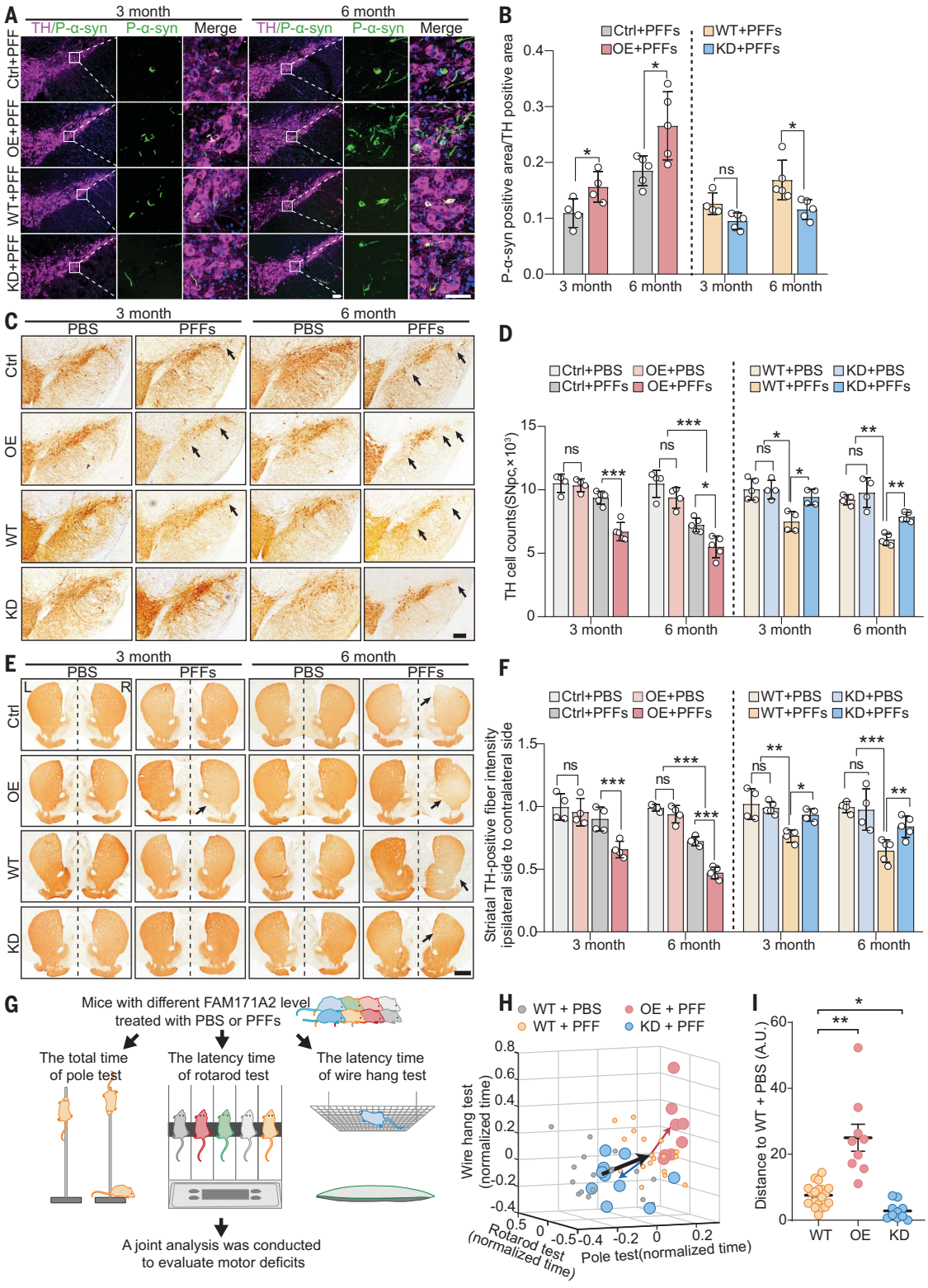

Fig. 2. FAM171A2 controls PFFs inoculation-induced α-syn pathology and neurotoxicity. (**A**) Representative images of double immunostaining for p-α-syn (green) and TH (magenta) in the SN of different groups 3 or 6 months after α-syn PFF treatment. Staining with 4′,6-diamidino-2-phenylindole (DAPI) is shown in blue. Scale bar, 100 μm. Insets show examples of higher magnification; scale bar, 50 μm. (**B**) Quantification of the ratio of p-α-syn–positive area to the TH-positive area in the SN on the PFF injection side (N = 4 to 5 mice per group, 6 brain sections per mouse). (**C**) Representative images of TH immunohistochemistry in SN sections from different groups 3 or 6 months after PBS or α-syn PFF treatment. Arrows indicate lesions. Scale bar, 200 μm. (**D**) Stereological counting of TH-positive neurons in the right SN of mice from the indicated experimental group (N = 4 to 5 mice per group, 7 to 9 brain sections per mouse). (**E**) Representative images of TH immunohistochemistry in striatum sections 3 or 6 months after PBS or α-syn PFF treatment. Arrows indicate lesions. Scale bar, 500 μm. (**F**) Quantification of TH fiber density in striatum determined by average optical density measurement (N = 4 to 5 mice per group). (**G**) Schematic of the motor function tests in different groups treated with PBS or α-syn PFFs at 6 months after treatments. (**H**) Three-dimensional (3D) scatterplot of the mice motor performance. The black arrow connects the centroid of the PBS-treated wild-type group to α-syn PFF-treated wild-type group. The red arrow indicates the distance between α-syn PFF-treated wild-type to the FAM171A2-overexpressing group. The blue arrow identifies the distance between α-syn PFF-treated wild-type to FAM171A2-knockdown groups. (**I**) Quantification of the Mahalanobis population vector distances toward the PBS-treated wild-type group 6 months after treatment in the 3D scatter plot shown in (H). In all panels, data are presented as mean ± SEM. For (I), one-way ANOVA with a Tukey's post-test was used. For panels B, D, and F, two-way ANOVA with a Tukey's post hoc test was used. ns, not significant; *P < 0.05; **P < 0.01; ***P < 0.001. Ctrl, control; OE, overexpression; WT, wild type; KD, knockdown; SNpc, substantia nigra pars compacta; L, left; R, right.

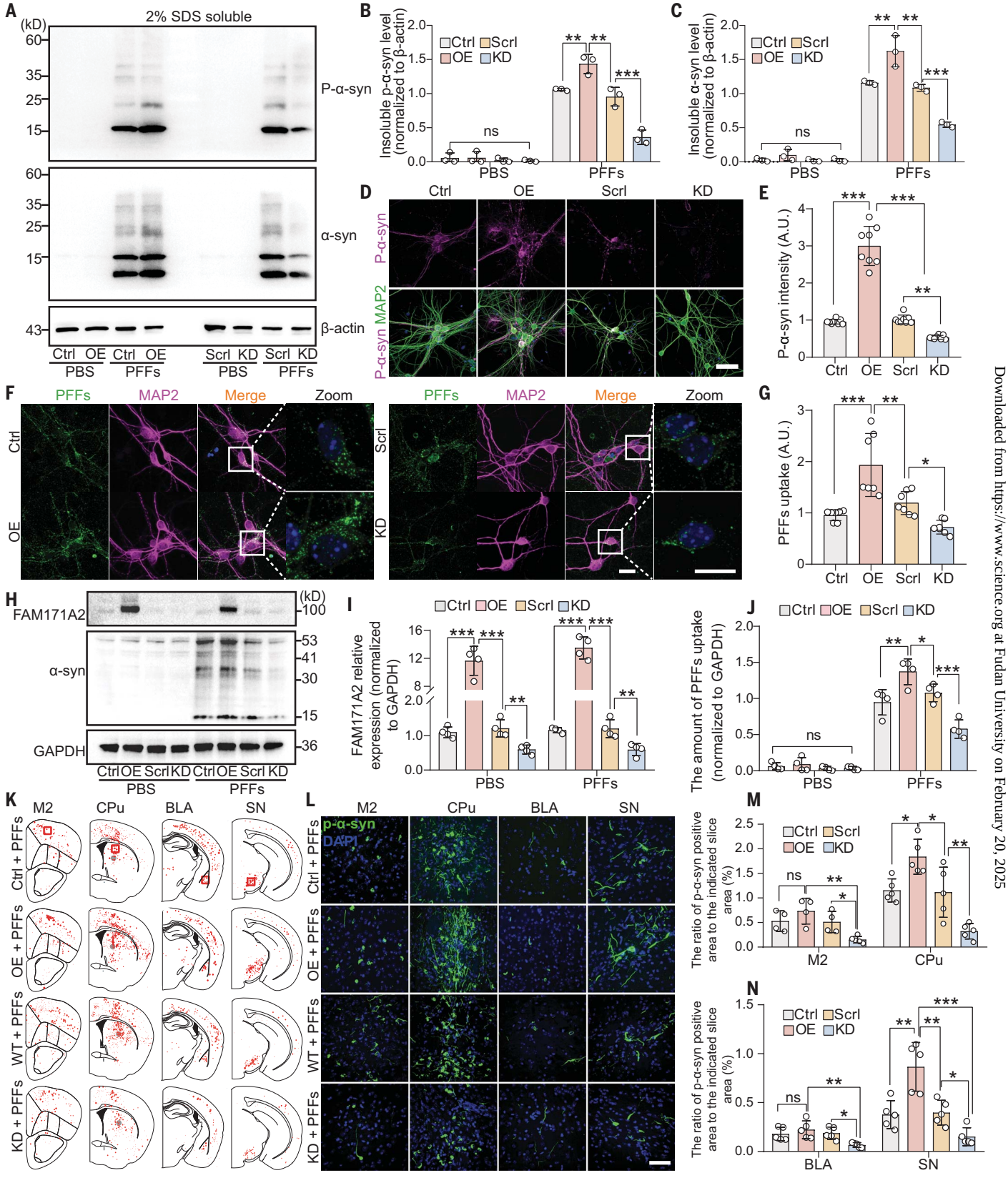

Fig. 3. FAM171A2 mediates α-syn endocytosis and regulates α-syn pathology spread. (**A**) Representative immunoblots of insoluble α-syn, p-α-syn, and β-actin in primary cortical neurons after PBS or α-syn PFF treatment in indicated groups. (**B** and **C**) Quantification of insoluble p-α-syn (B) and α-syn (C) amounts in (A). *N* = 3 independent experiments. (**D**) Representative p-α-syn (magenta) immunofluorescence images in primary cortical neurons with different FAM171A2 amounts after treatment with α-syn PFFs for 14 days. MAP2, green; DAPI, blue. *N* = 8 independent experiments. Scale bar, 20 μm. (**E**) Quantification of p-α-syn

immunofluorescence. (**F**) Representative images of α-syn PFF uptake in indicated groups 3 hours after incubation with α-syn PFFs-488; *N* = 7 independent experiments. The insets show examples of higher magnification; scale bars, 20 μm. (**G**) Quantification of the amount of internalized α-syn PFFs in (F). (**H**) Western blots showing the expression of FAM171A2 and the amount of α-syn PFF uptake in different groups of primary cortical neurons 3 hours after incubation with either α-syn PFFs or PBS. Glyceraldehyde-3-phosphate dehydrogenase (GAPDH) is blotted as loading controls. (**I** and **J**) Quantification of the expression of FAM171A2 (I) and the amount of α-syn PFF uptake (J) in (H). *N* = 4 independent experiments. (**K**) Representative distribution of p-α-syn pathology (red dots) on several coronal sections in different groups 6 months after α-syn PFF treatment. Gray circles denote injected sites. (**L**) Representative images of p-α-syn pathology on M2, CPu, BLA, and SN regions in the red boxes in (K). Scale bar, 20 μm. (**M** and **N**) Quantification of the percentage of the p-α-syn occupied area to the total area of the corresponding slice on the PFFs injection side. *N* = 4 to 5 mice per group. For (B), (C), (I), and (J), a two-way ANOVA with a Tukey's post hoc test was performed. For (E), (G), (M), and (N), a one-way ANOVA with a Tukey's post hoc test was performed. In all panels, data are expressed as mean ± SEM. ns, not significant; **P* < 0.05; ***P* < 0.01; ****P* < 0.001. Ctrl, control; OE, FAM171A2 overexpression; Scrl, scramble control; KD, FAM171A2 knockdown; WT, wild type.

by SDS–polyacrylamide gel electrophoresis analysis (fig. S3B). In addition, these α-syn PFFs were fully capable of inducing the formation of phospho-Ser^{129} α-syn (p-α-syn)–positive inclusions (fig. S3C), a feature indicative of pathological misfolding of α-syn (*17*, *18*). To manipulate FAM171A2, we developed FAM171A2 overexpression and knockdown mouse models. Injection of adeno-associated viruses (AAVs) into the right SN increased the expression of FAM171A2 protein (fig. S4, A to F). In addition, we utilized the CRISPR-Cas9 genome editing system to delete the exons 4 to 7 in *FAM171A2* gene. Because of the lethality of homozygous FAM171A2 knockouts, heterozygous mice (*FAM171A2*$^{+/-}$) were used for this study; these animals showed no evident morphological or behavioral abnormalities (fig. S4, E to N).

Injection of α-syn PFFs (2 μg/μl) into the right dorsal striatum resulted in uptake of PFFs through axonal terminals (fig. S5), leading to accumulation of α-syn PFFs in the ipsilateral SN. Three or 6 months after inoculation, we found that FAM171A2 overexpression led to an increased p-α-syn pathology in SN compared with control mice, whereas FAM171A2 knockdown reduced the accumulation of p-α-syn pathology compared with controls (Fig. 2, A and B). Previous work showed that p-α-syn pathology produces toxicity to tyrosine hydroxylase (TH)–positive dopaminergic neurons, leading to motor dysfunction in PD (*19*, *20*). Having found that FAM171A2 controlled the accumulation of p-α-syn pathology in SN, we next examined the impact of FAM171A2 amounts on α-syn PFF–induced neurotoxicity. Consistent with the effect on α-syn pathology, FAM171A2 overexpression led to a more pronounced loss of TH-positive neurons and fiber degeneration, whereas FAM171A2 knockdown was neuroprotective (Fig. 2, C to F). Furthermore, pole test, rotarod test, and wire hang test revealed that FAM171A2 overexpression worsened α-syn PFF–induced behavior deficits, whereas FAM171A2 knockdown showed performance similar to that measured in wild-type mice (Fig. 2, G to I, and fig. S6). To directly test the necessity of FAM171A2 of neuronal origin for α-syn PFF–induced pathology, we developed a mouse model with neuronal-specific knockout of FAM171A2 (Nes-Cre^{+}: *FAM171A2*$^{flox/flox}$; fig. S4, E and F). Following a 3-month incubation period with α-syn PFFs, the neuron-specific knockout of FAM171A2 reproduced all the protective phenotypes observed in the whole-body knockdown mice (fig. S7). Taken together, our findings indicate that neuronal FAM171A2 bidirectionally modulates the accumulation of α-syn pathology and affects PFFs neurotoxicity.

FAM171A2 mediates the endocytosis of α-syn fibrils

We next used an in vitro cellular model to study the mechanism underlying FAM171A2's regulation on α-syn pathology. Primary cortical neurons were transfected with AAV to either overexpress or knockdown FAM171A2 (fig. S8). Following a 14-day incubation with 2 μg/ml of α-syn PFFs, we assessed the pathological α-syn contents in the neurons. Consistent with the in vivo findings, increase in insoluble p-α-syn and total insoluble α-syn amounts were detected in neurons overexpressing FAM171A2, whereas FAM171A2 knockdown resulted in a marked reduction of p-α-syn and α-syn (Fig. 3, A to E). We observed similar effects when incubation of α-syn PFFs preceded FAM171A2 manipulation (fig. S9). The ratio of insoluble p-α-syn to total insoluble α-syn was not affected by FAM171A2 manipulation (fig. S10A), indicating no effect of FAM171A2 on the phosphorylation propensity of α-syn. Moreover, neurons treated with phosphate-buffered saline (PBS) instead of α-syn PFFs showed similar endogenous soluble α-syn expression with or without FAM171A2 manipulations (fig. S10, B to E), suggesting that FAM171A2 did not influence the equilibrium between endogenous α-syn production and degradation. Given these results, we hypothesized that FAM171A2 might regulate the internalization of extracellular α-syn fibrils.

To test our hypothesis, we used a short incubation assay of fluorescently labeled α-syn PFFs (Alexa-Flour 488) in primary neurons under different conditions (FAM171A2 overexpression or knockdown). FAM171A2 overexpression enhanced the uptake of α-syn PFFs compared with wild-type neurons as determined by immunofluorescence and western blot. By contrast, FAM171A2 knockdown led to a substantial reduction in the uptake compared with control neurons (fig. 3, F to J). Internalized α-syn PFFs and FAM171A2 colocalized with transferrin, an indicator substrate for clathrin-mediated endocytosis (CME), and with cholera toxin B, a marker for caveolae-mediated endocytosis (CvME) (fig. S11), consistent with prior reports suggesting that α-syn PFFs are internalized through endocytosis (*8*, *21*, *22*). To directly test the necessity of endocytic pathways, we used dynasore, an inhibitor targeting CME, and MβCD, an inhibitor of CvME. We observed that the heightened α-syn PFF endocytosis caused by FAM171A2 overexpression was effectively abolished by both these inhibitors, indicating that these two pathways are necessary for FAM171A2-mediated internalization of α-syn PFFs (fig. S12). Thus, these results suggest that FAM171A2 might regulate the endocytosis of α-syn PFFs.

To test whether FAM171A2 may affect the spread of α-syn pathology between neurons, we performed in vivo studies measuring the brain distribution of p-α-syn pathology 6 months after α-syn PFF inoculation in mice with either overexpression or knockdown of FAM171A2. We examined key brain regions known to be implicated in this model, including the SN, secondary motor cortex (M2), basolateral amygdala (BLA), and striatum region (CPu). FAM171A2 overexpression led to an increase in p-α-syn pathology in SN and CPu compared with that in wild-type animals (Fig. 3, K to N). In addition, whole-body as well as neuronal FAM171A2 knockdown reduced the spread of p-α-syn pathology across all four brain regions (Fig. 3, K to N, and fig. S13). Together, these data indicate that neuronal FAM171A2 controls the endocytosis of α-syn fibrils and also regulates the spread of α-syn pathology in the brain.

FAM171A2 directly binds α-syn fibrils

To visualize the FAM171A2-mediated endocytosis of α-syn PFFs, we used total internal reflection microscopy (TIRF) (movie S1). In N2a cells expressing dTomato-tagged FAM171A2, we observed that most α-syn PFFs (we used α-syn PFFs-488; see materials and methods) colocalized with FAM171A2-positive puncta (Fig. 4A). Furthermore, we investigated the disappearance of α-syn PFF puncta from the plasma membrane, indicative of their internalization into cells. Our findings revealed that 79% of α-syn PFF disappearance events happened in puncta with FAM171A2-positive labeling (Fig. 4A, fig. S14, and movie S2), suggesting that FAM171A2-mediated endocytosis is among the main routes of α-syn

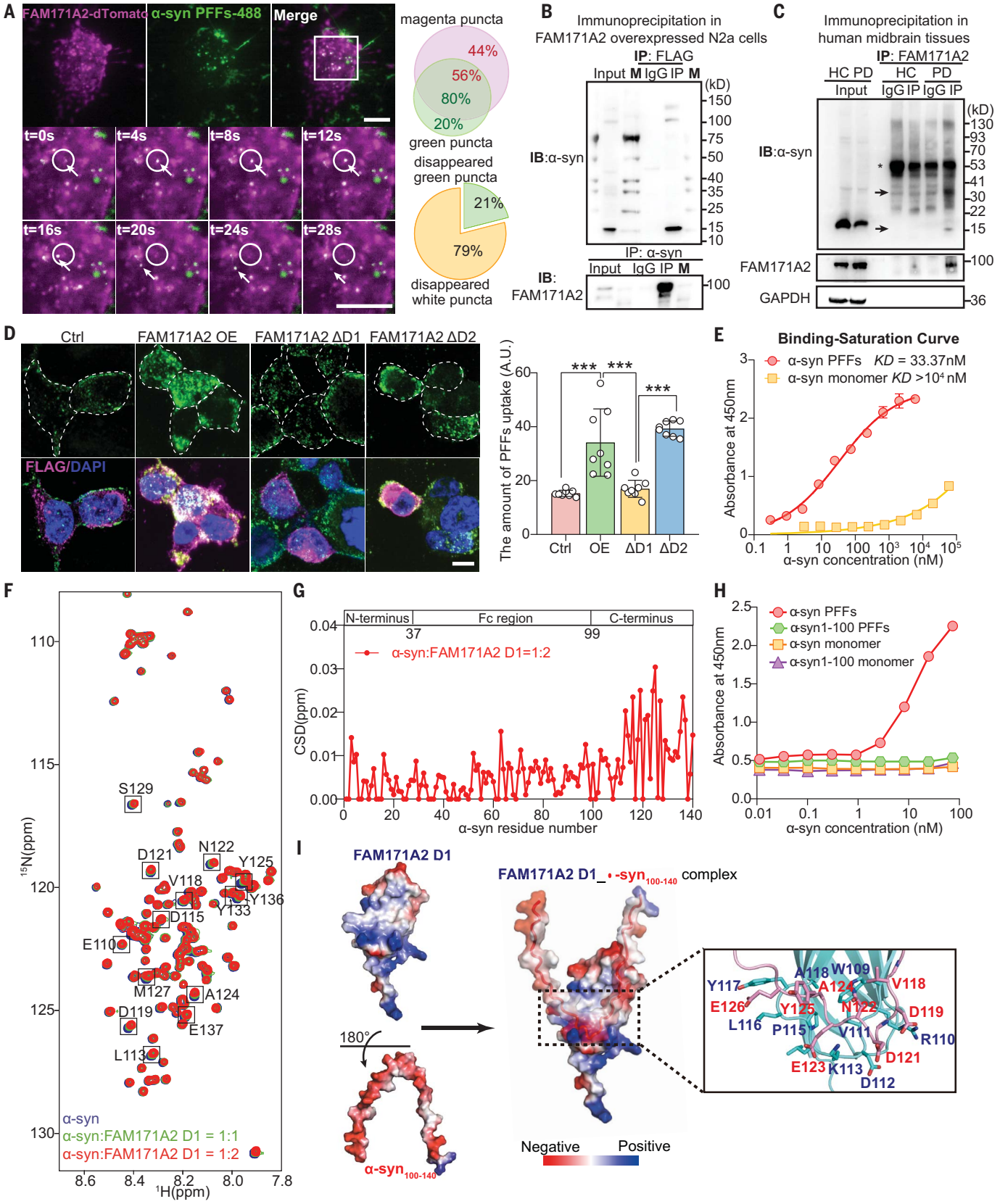

Fig. 4. FAM171A2 directly interacts with α-syn fibrils. (**A**) Representative TIRF images showing colocalization of α-syn PFFs (green) with FAM171A2 (magenta) in N2a cells transfected with FAM171A2-dTomato. Insets show examples of higher magnification of FAM171A2 and α-syn PFFs-488 (indicated by white arrows) at different times. The white circle is in a fixed position. Scale bars, 5 μm. The upper right panel shows the Venn diagram for FAM171A2 puncta and α-syn PFFs-488 puncta in all imaged cells. The lower right panel presents the proportion of single labeled puncta in disappeared α-syn PFFs. (**B**) Coimmunoprecipitation blots testing the interaction between α-syn PFFs and FAM171A2 in N2a cells

overexpressing FAM171A2-FLAG. (**C**) Coimmunoprecipitation testing the interaction between α-syn and FAM171A2 from the postmortem midbrain tissues of controls and individuals with PD. The asterisk represents a nonspecific band; arrows indicate possible α-syn bands. *N* = 2 controls and 2 patients with PD. (**D**) Representative images showing the amount of α-syn PFFs binding to HEK293 cells transfected with full-length or truncated FAM171A2-FLAG. Scale bar, 10 μm. The right panel shows quantification of PFFs fluorescence as mean ± SEM. *N* = 8 independent experiments. A one-way ANOVA followed by Tukey's post hoc test for multiple comparisons was performed. (**E**) The binding curves for α-syn PFFs or monomers to FAM171A2 domain 1 protein fitted to logistic functions. *N* = 3 independent experiments. (**F**) Overlay of the 2D ^{1}H-^{15}N HSQC spectra of ^{15}N-labeled α-syn alone (blue) and in the presence of FAM171A2 domain 1 protein at molar ratios of 1:1 (green) or 1:2 (red). Black boxes show residues in α-syn with significant CSDs. (**G**) CSDs of α-syn in the presence of FAM171A2 domain 1 protein at the molar ratio of 1:2. Fc, crystallizable fragment. (**H**) Binding affinity of FAM171A2 domain 1 protein with different α-syn forms tested by ELISA assay. *N* = 3 independent experiments. (**I**) Predicted electrostatic surface model of the α-syn$_{100–140}$ residues in complex with FAM171A2 domain 1. The model confidence is 0.38. M, marker; IP, immunoprecipitation; IB, immunoblotting; FAM171A2 ΔD1, FAM171A2 domain 1 deletion; FAM171A2 ΔD2, FAM171A2 domain 2 deletion. Single-letter abbreviations for the amino acid residues referenced throughout the figures are as follows: S, Ser; N, Asn; D, Asp; V, Val; Y, Tyr; G, Gly; E, Glu; M, Met; A, Ala; L, Leu; W, Trp; R, Arg; K, Lys; P, Pro.

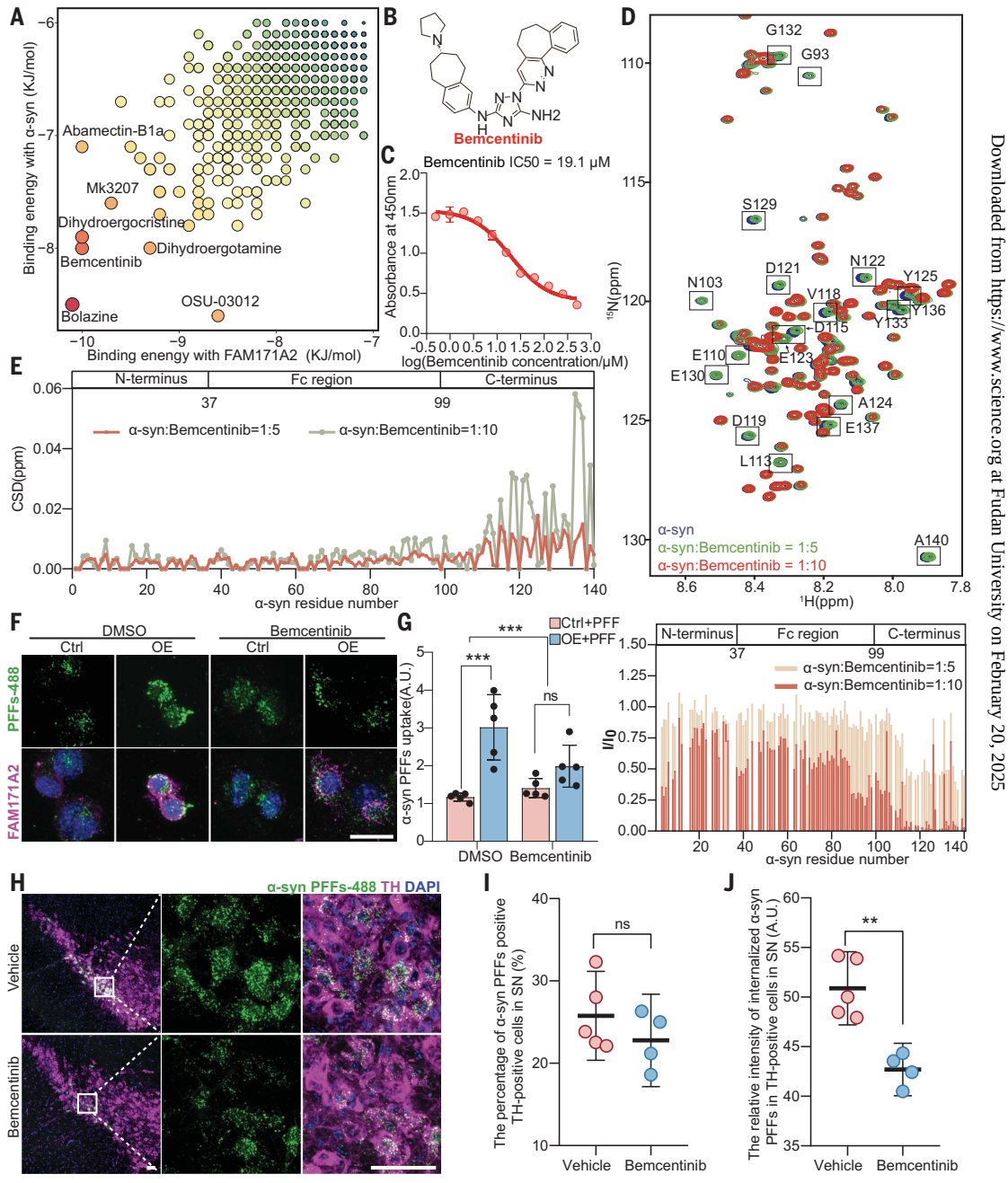

Fig. 5. Blocking the interaction between FAM171A2 and α-syn fibrils by bemcentinib prevents α-syn fibril uptake. (**A**) Binding energies of compounds to FAM171A2 and α-syn binding sites predicted by MTiOpenScreen. (**B**) The chemical structure of bemcentinib. (**C**) The inhibition activity curve for bemcentinib to block the binding of FAM171A2 domain 1 protein and α-syn PFFs. *N* = 3 independent experiments. (**D**) Overlay of the 2D ^{1}H-^{15}N HSQC spectra of 20-μM ^{15}N-labeled α-syn alone (blue) and in the presence of bemcentinib protein at molar ratios of 1:5 (green) or 1:10 (red). Black boxes around individual amino acids show the residues of α-syn with significant CSDs. The lower panel shows the residue-specific intensity ratio (I/I_0) of α-syn titrated by bemcentinib at different ratios. (**E**) CSDs of α-syn in the presence of bemcentinib at a molar ratio of 1:5 or 1:10. The domain organization of α-syn is shown on top. (**F**) Representative immunofluorescence images showing the uptake of α-syn PFFs in FAM171A2-overexpressed or control N2a cells. Scale bar, 20 μm. (**G**) Quantified data of the amount of α-syn PFF uptake in (F). Data are expressed as means ± SEM; *N* = 5 independent experiments, compared by two-way ANOVA with a Tukey's post hoc test for multiple comparisons. (**H**) Representative images showing the uptake of α-syn PFFs-488 by TH-positive neurons in SN after receiving a 7-day treatment with vehicle or bemcentinib. The insets show examples at higher magnification. Scale bars = 50 μm. (**I**) Quantification of the percentage of α-syn PFFs-488–positive, TH-positive neurons in the SN in indicated experiment groups. Data are expressed as means ± SEM; *N* = 4 to 5 mice per group, compared by unpaired *t* test. (**J**) Quantification of the relative mean intensity of α-syn PFFs-488 in the SN in indicated experiment groups. Data are expressed as means ± SEM; *N* = 4 to 5 mice per group, compared by unpaired *t* test. ns, not significant; $^{**}P < 0.01$; $^{***}P < 0.001$. ppm, parts per million.

PFF internalization. Immunoprecipitation experiments in N2a cells showed that molecular interaction exists between FAM171A2 and α-syn PFFs (Fig. 4B). Similar immunoprecipitation experiments in freshly frozen postmortem human midbrain tissues showed binding between FAM171A2 and α-syn in samples from individuals with PD but not in brains from healthy controls (Fig. 4C). These findings support the interaction between FAM171A2 and pathological α-syn in both preclinical models and in clinical samples.

To locate the binding site of α-syn on FAM171A2, we measured the binding of α–syn PFFs to the cell surface in human embryonic kidney (HEK) 293 cells overexpressing full-length or domain-truncated FAM171A2 (domain 1, amino acids 30 to 125, and domain 2, amino acids 126 to 315). We found that FAM171A2 domain 1 is necessary for the uptake of α-syn PFFs (Fig. 4D). We then purified the FAM171A2 domain 1 and established an enzyme-linked immunosorbent assay (ELISA). Domain 1 of FAM171A2 binds to α-syn PFFs with high affinity [estimated equilibrium dissociation constant (K_D) around 33 nM], which was about three orders of magnitude stronger than that measured from monomeric α-syn (Fig. 4E). On the other hand, tau and amyloid β (Aβ) monomers or fibrils showed lower or no affinity to FAM171A2 domain 1 (fig. S15). Incubating FAM171A2-overexpressing N2a cells with purified FAM171A2 domain 1 proteins blocked the internalization of α-syn PFFs (fig. S16), further verifying the binding between FAM171A2 domain 1 and α-syn PFFs. We further dissected the molecular interactions between FAM171A2 domain 1 and α-syn using nuclear magnetic resonance (NMR) spectroscopy. By labeling the nitrogen atoms in α-syn with ^{15}N, we were able to map individual amino acid residues with the ^{1}H-^{15}N heteronuclear single-quantum coherence (HSQC) spectrum (*23*). When we titrated the solution with purified FAM171A2 domain 1, we observed chemical shift deviations (CSDs) in C-terminal residues of α-syn (Fig. 4, F and G, and fig. S17), suggesting a potential binding site. Consistently, deleting the C-terminal region of α-syn (amino acids 101 to 140) completely abolished the binding to FAM171A2 domain-1 (Fig. 4H).

We then used AlphaFold-Multimer to predict the structure of the FAM171A2–α-syn complex. The resulting structure revealed that the negatively charged α-syn C terminus (Val^{118}, Asp^{119}, Asp^{121}, Asn^{122}, Glu^{123}, Ala^{124}, Tyr^{125}, Glu^{126}) aligned with the positively charged surface of FAM171A2 domain-1 (Trp^{109}, Arg^{110}, Val^{111}, Asp^{112}, Lys^{113}, Pro^{115}, Leu^{116}, Tyr^{117}, Ala^{118}) (Fig. 4I). The predicted interacting residues on α-syn were closely aligned with those that showed chemical shift deviations in our NMR titration experiments, indicating a faithful representation of the binding interface. Binding of FAM171A2 to the α-syn C terminus could potentially explain the selective affinity of FAM171A2 toward α-syn fibrils, as our previous study found that the α-syn C-terminal region was partially shielded in monomers (*24*) but fully exposed and densely packed in fibrils (*25*). Altogether, our data demonstrated specific binding between FAM171A2 and α-syn PFFs, providing the structural basis for FAM171A2-mediated α-syn uptake.

Bemcentinib blocks binding between α-syn fibrils and FAM171A2

With the predicted complex structure, we performed a virtual screening to identify potential interfering small molecules with the Drug-lib database in MTiOpenScreen (*26*). We reasoned that candidate molecules should show high affinity to the same binding site, thus blocking interaction between FAM171A2 and α-syn through competition. We screened a collection of 7173 previously approved drugs and found 7 compounds (bolazine, bemcentinib, dihydroergocristine, Mk3207, dihydroergotamine, OSU-03012, and abamectin-B1a) with high docking affinities to interacting residues from both FAM171A2 and α-syn (Fig. 5A). We measured six out of the seven molecules for their effects in inhibiting the interaction between FAM171A2 domain 1 and α-syn PFFs with our ELISA approach and found that bemcentinib, a drug developed for cancer treatment (*27*), showed a strong effect at micromolar concentrations (Fig. 5, B and C, and fig. S18A). To gain structural insights underlying the effects of bemcentinib, we conducted NMR spectroscopy experiments using titration of bemcentinib to the ^{15}N-labeled α-syn monomer solution. Bemcentinib caused a marked drop in the HSQC signal intensity and substantial CSDs in the C terminus of α-syn, with many affected residues matching those found to be the interaction sites to FAM171A2 domain 1 (Fig. 5, D and E). These data suggest that bemcentinib might interfere with FAM171A2–α-syn interaction by competing overlapping residues.

We then examined whether bemcentinib could suppress the endocytosis of α-syn PFFs. We first measured the effect of bemcentinib in N2a cells with FAM171A2 overexpression. Pretreating N2a cells with 10-μM bemcentinib for 1 hour reduced the amount of α-syn binding to FAM171A2 and endocytosed into the cells (Fig. 5, F and G, and fig. S18B) but showed no effect in cells without FAM171A2 overexpression, indicating a potent effect in blocking FAM171A2-mediated endocytosis of α-syn PFFs. To test the effect of bemcentinib in vivo, we developed a liquid chromatography detection method for bemcentinib and found that bemcentinib could not cross the blood-brain barrier (*28*, *29*) (fig. S19). Therefore, we treated wild-type mice that previously received 2.5 μl of α-syn PFFs-488 (2 μg/ml) in the right striatum, with 5 μl of bemcentinib solution (2.5 mg/ml) injected in the right lateral ventricle for 7 consecutive days. Bemcentinib did not cause obvious toxicity to neurons (fig. S20) or abnormal behavior in treated mice. However, bemcentinib reduced the total amount of internalized α-syn PFFs-488 in the right SN (Fig. 5, H to J). Together, these findings suggest that bemcentinib might inhibit the binding between FAM171A2 and α-syn PFFs in vivo, thus representing a potential strategy to block the pathological spread of α-syn fibrils in the context of PD.

Discussion

Several membrane proteins, such as heparan sulfate proteoglycan (*12*), low-density lipoprotein receptor–related protein 1 (*11*), lymphocyte-activation gene 3 (*10*), Mer tyrosine kinase (*30*), and glycoprotein nonmetastatic melanoma protein B (*31*), have been proposed as potential mediators in the recognition of pathological α-syn. Despite the keen interest in identifying such a mediator, these proteins currently lack clear evidence for neuronal expression, selectivity for α-syn fibril over monomers, or in vivo efficacy (*11*, *12*, *32*). Our findings identify a binding site between FAM171A2 and α-syn and provide strong evidence suggesting that FAM171A2 has stronger binding affinity to α-syn fibrils compared with that of monomers. FAM171A2 is expressed on SN neurons in humans, with elevated expression and binding with α-syn fibrils detected in individuals with PD compared with controls. Altogether, our data suggest that FAM171A2 is a receptor that directly binds with α-syn fibrils and controls the neuronal uptake of them (fig. S21).

PD is predominantly marked by motor impairments due to the gradual degeneration of dopaminergic neurons in SN. The exact neural mechanisms responsible for the development of PD remain elusive, but the spread of pathological α-syn across different brain regions is closely linked to the disease's progression (*3*, *33*), suggesting a fundamental role in its pathogenesis. Currently, the specific molecular processes that facilitate the distribution of pathological α-syn are not fully understood. In this work, we identified a potential target for limiting the spread of α-syn fibrils between neurons. We pinpointed the specific subdomain of FAM171A2 and the corresponding interface on α-syn responsible for their direct interaction, identifying the key residues involved. Moreover, we identified bemcentinib, which interferes with the amino acids critical for the FAM171A2–α-syn interaction and demonstrated bemcentinib's ability to prevent the FAM171A2 and α-syn PFF binding and to block the uptake of α-syn PFFs in mice. Although bemcentinib may not be directly applicable in a clinical setting owing to its low efficacy in brain penetrance, our method of using structural analysis opens the possibility to discover effective drugs based on our findings. Altogether, we identified a pathway potentially involved in the spread of α-syn fibrils between brain areas and suggest a compelling strategy for impeding this process in individuals with PD.

REFERENCES AND NOTES

1. B. R. Bloem, M. S. Okun, C. Klein, *Lancet* **397**, 2284–2303 (2021).
2. H. R. Morris, M. G. Spillantini, C. M. Sue, C. H. Williams-Gray, *Lancet* **403**, 293–304 (2024).
3. M. Carceles-Cordon, D. Weintraub, A. S. Chen-Plotkin, *Neuron* **111**, 1531–1546 (2023).
4. M. X. Henderson *et al*., *Nat. Neurosci.* **22**, 1248–1257 (2019).
5. D. J. Surmeier, J. A. Obeso, G. M. Halliday, *Nat. Rev. Neurosci.* **18**, 101–113 (2017).
6. C. Peng, J. Q. Trojanowski, V. M. Y. Lee, *Nat. Rev. Neurol.* **16**, 199–212 (2020).
7. N. Uemura, M. T. Uemura, K. C. Luk, V. M. Y. Lee, J. Q. Trojanowski, *Trends Mol. Med.* **26**, 936–952 (2020).
8. Q. Zhang *et al*., *Proc. Natl. Acad. Sci. U.S.A.* **117**, 10865–10875 (2020).
9. S. H. Oh *et al*., *Cell Rep.* **14**, 835–849 (2016).
10. X. Mao *et al*., *Science* **353**, aah3374 (2016).
11. K. Chen *et al*., *Mol. Neurodegener.* **17**, 57 (2022).
12. B. B. Holmes *et al*., *Proc. Natl. Acad. Sci. U.S.A.* **110**, E3138–E3147 (2013).
13. W. Xu *et al*., *Sci. Adv.* **6**, eabb3063 (2020).
14. C. Xiang *et al*., *NPJ Parkinsons Dis.* **8**, 165 (2022).
15. K. C. Luk *et al*., *Science* **338**, 949–953 (2012).
16. L. A. Volpicelli-Daley *et al*., *Neuron* **72**, 57–71 (2011).
17. C. Quadalti *et al*., *Nat. Med.* **29**, 1964–1970 (2023).
18. N. Uemura *et al*., *Mol. Neurodegener.* **13**, 21 (2018).
19. J. Blesa, G. Foffani, B. Dehay, E. Bezard, J. A. Obeso, *Nat. Rev. Neurosci.* **23**, 115–128 (2022).
20. A. Tozzi *et al*., *Brain* **144**, 3477–3491 (2021).
21. I. Kawahata *et al*., *Biomedicines* **9**, 49 (2021).
22. T.-Y. Ha *et al*., *Mol. Brain* **14**, 122 (2021).
23. Z. Liu *et al*., *J. Biol. Chem.* **293**, 14880–14890 (2018).
24. S. Zhang *et al*., *Proc. Natl. Acad. Sci. U.S.A.* **118**, e2011196118 (2021).
25. Y. Li *et al*., *Cell Res.* **28**, 897–903 (2018).
26. C. M. Labbé *et al*., *Nucleic Acids Res.* **43**, W448-54 (2015).
27. S. J. Holland *et al*., *Cancer Res.* **70**, 1544–1554 (2010).
28. R. Cecchelli *et al*., *Nat. Rev. Drug Discov.* **6**, 650–661 (2007).
29. P. Jeffrey, S. Summerfield, *Neurobiol. Dis.* **37**, 33–37 (2010).
30. M.-F. Dorion *et al*., *Brain* **147**, 427–443 (2024).
31. M. E. Diaz-Ortiz *et al*., *Science* **377**, eabk0637 (2022).
32. M. Emmenegger *et al*., *EMBO Mol. Med.* **13**, e14745 (2021).
33. C. Smith *et al*., *J. Neurol. Neurosurg. Psychiatry* **90**, 1234–1243 (2019).
34. D. Chang *et al*., *Nat. Genet.* **49**, 1511–1516 (2017).

ACKNOWLEDGMENTS

We extend our heartfelt gratitude to the participants and researchers involved in the UK Biobank, the PDWBS study, the PDGene study, the FinnGen study, and the PPMI cohort databases. We extend our sincere gratitude to L. Ma for her valuable suggestions for this study. We also express our appreciation to J. Shen from Shimadzu Corporation for his invaluable experimental support. Special thanks are due to all members of Dr. Yu's laboratory for their unwavering support, assistance, and guidance. Lastly, we express our profound appreciation to all the patients who generously donated their brain, blood, or CSF samples for research purposes. **Funding:** STI2030-Major Projects (2022ZD0211600) (J.-T.Y.); National Natural Science Foundation of China (82071201, 82271471, and 92249305) (J.-T.Y.); Shanghai Municipal Science and Technology Major Project (2023SHZDZX02) (J.-T.Y.); Excellent Academic Research Leader Program of Shanghai (23XD1420400) (J.-T.Y.); Emerging Interdisciplinary Research Project of Shanghai (2022JC014) (J.-T.Y.); Research Start-up Fund of Huashan Hospital (2022QD002) (J.-T.Y.); National Natural Science Foundation of China (82188101, 22425704, and 32171236) (C.L.); the CAS Project for Young Scientists in Basic Research (YSBR-095) (C.L.); the Strategic Priority Research Program of the Chinese Academy of Sciences (XDB106000) (C.L.); STI2030-Major Project no. 2021ZD0201100 Task 4 no. 2021ZD0201104 (W.-S.L.); China Postdoctoral Science Foundation (2023M740682) (K.-M.W.); Postdoctoral Fellowship Program of CPSF (GZC20230506) (K.-M.W.); National Natural Science Foundation of China (82401676) (K.-M.W.); Shanghai Pilot Program for Basic Research – FuDan University 21TQ1400100 (22TQ019) (P.Y.); National Natural Science Foundation of China (32371036) (P.Y.). J.-T.Y. was additionally supported by ZHANGJIANG LAB; Tianqiao and Chrissy Chen Institute; and the State Key Laboratory of Neurobiology and Frontiers Center for Brain Science of Ministry of Education, Fudan University. C.L. was additionally supported by Shanghai Basic Research Pioneer Project and the Shanghai Pilot Program for Basic Research, Chinese Academy of Science, Shanghai Branch. C.L. is a SANS Exploration Scholar. **Author contributions:** Conceptualization: J.-T.Y., P.Y., K.-M.W.; Methodology: K.-M.W., Q.-H.X., Y.-Q.L., Y.-W.F., S.-D.H., Z.-F.Y., T.-T.W., M.C., L.Y., Y.-J.X., Y.-S.S., C.L., P.Y.; Data curation: K.-M.W., Y.-R.Z., S.-D.C., Y.G., B.-S.W., L.-Z.M.; Investigation: K.-M.W., Q.-H.X.; Visualization: K.-M.W., Y.Z., Y.-L.C., P.Y.; Resources: J.W., J.Z., S.-F.C., W.-D.L., W.-S.L., J.-T.Y., C.L., P.Y.; Funding acquisition: J.-T.Y., P.Y., C.L., K.-M.W., W.-S.L.; Project administration: J.-T.Y., P.Y.; Supervision: J.-T.Y.; Writing – original draft: K.-M.W., P.Y., J.-T.Y.; Writing – review and editing: B.-X.L., W.-D.L., K.Y., J.-Y.L. **Competing interests:** K.-M.W., P.Y., and J.-T.Y. are inventors on a patent application (PCT/CN2025/071237) submitted by Huashan Hospital, Fudan University, that covers potential strategies in suppressing FAM171A2 or blocking FAM171A2–α-syn interaction as potential treatment for neurodegenerative diseases. **Data and materials availability:** Individual-level genotype data described in this study are available to bona fide researchers per the UK Biobank data access protocol (https://www.ukbiobank.ac.uk/enable-your-research/apply-for-access). Summary statistics for the top 9830 variants from Chang *et al*. (2017) (*34*) is available at http://research-pub.gene.com/chang_et_al_2017/. FinnGen data are available at https://risteys.finngen.fi/. PPMI data are publicly available to bona fide researchers upon application at https://www.ppmi-info.org/. All data presented in the article are available in data S1.

SUPPLEMENTARY MATERIALS

science.org/doi/10.1126/science.adp3645
Materials and Methods
Figs. S1 to S21
Tables S1 to S4
References (*35*–*47*)
MDAR Reproducibility Checklist
Movies S1 and S2
Data S1

Submitted 22 March 2024; resubmitted 21 October 2024
Accepted 10 January 2025
10.1126/science.adp3645